Inorganic Chemistry
Article

Inorg. Chem. **2011**, *50*, 1295–1303 **1295**
DOI: 10.1021/ic102228u

Curcumin as the OO Bidentate Ligand in "2 + 1" Complexes with the $[M(CO)_3]^+$ (M = Re, ^{99m}Tc) Tricarbonyl Core for Radiodiagnostic Applications

Marina Sagnou,[†] Dimitra Benaki,[†] Charalampos Triantis,[‡] Theodoros Tsotakos,[‡] Vassilis Psycharis,[§] Catherine P. Raptopoulou,[§] Ioannis Pirmettis,[‡] Minas Papadopoulos,[‡] and Maria Pelecanou*[,†]

[†]*Institute of Biology,* [‡]*Institute of Radioisotopes/Radiodiagnostic Products, and* [§]*Institute of Materials Science, National Centre for Scientific Research "Demokritos", 15310 Athens, Greece*

Received September 13, 2010

The synthesis and characterization of "2 + 1" complexes of the $[M(CO)_3]^+$ (M = Re, ^{99m}Tc) core with the β-diketones acetylacetone (complexes **2**, **8**) and curcumin (complexes **5**, **10** and **6**, **11**) as bidentate OO ligands, and imidazole or isocyanocyclohexane as monodentate ligands is reported. The complexes were synthesized by reacting the $[NEt_4]_2[Re(CO)_3Br_3]$ precursor with the β-diketone to generate the intermediate aqua complex *fac*-$Re(CO)_3(OO)(H_2O)$ that was isolated and characterized, followed by replacement of the labile water by the monodentate ligand. All complexes were characterized by mass spectrometry, NMR and IR spectroscopies, and elemental analysis. In the case of complex **2**, bearing imidazole as the monodentate ligand, X-ray analysis was possible. The chemistry was successfully transferred at ^{99m}Tc tracer level. The curcumin complexes **5** and **6**, as well as their intermediate aqua complex **4**, that bear potential for radiopharmaceutical applications due to the wide spectrum of pharmacological activity of curcumin, were successfully tested for selective staining of β-amyloid plaques of Alzheimer's disease. The fact that the complexes maintain the affinity of the mother compound curcumin for β-amyloid plaques prompts for further exploration of their chemistry and biological properties as radioimaging probes.

Introduction

Recently, the synthesis and characterization of the neutral "2 + 1" mixed ligand complex *fac*-$M(CO)_3$(acac)(isc) (M = Re, ^{99m}Tc) with the β-diketone acetylacetone (in the form of acetylacetonate, acac) as the bidentate ligand and the isocyanocyclohexane (isc) as the monodentate ligand were reported by our group,[1] in the exploration of the acetylacetone bidentate OO system toward the development of target specific Re and ^{99m}Tc complexes. Our work extended the work of Benny et al.[2] that reported the synthesis of the *fac*-$Re(CO)_3$(acac)(pyr) complex with acetylacetone and pyridine (pyr) as the monodentate ligand. In continuation of our studies on β-diketones, we report the synthesis of the analogous *fac*-$M(CO)_3$(acac)(imi) complex **2** (Figure 1) with acetylacetone and imidazole (imi) as modentate ligand. Furthermore, and using the acac complexes (**2** and *fac*-$M(CO)_3$(acac)(isc)[1]) as models, we present the application of the synthesis and characterization procedures to the natural β-diketone curcumin (**3**, curcu) to prepare the "2 + 1" complexes *fac*-$M(CO)_3$(curcu)(imi) **5** and *fac*-$M(CO)_3$(curcu)(isc) **6** (Figure 2) with imidazole and isocyanocyclohexane as monodentate ligands, respectively.

Curcumin is the active ingredient in the herbal remedy and dietary spice turmeric derived from the rhizome of the herb *Curcuma longa*, commonly known as turmeric.[3] The rhizome of turmeric has been crushed into a vibrant orange-yellow powder and used in traditional medicines of China and India to dress wounds and treat infections, bites, burns, and skin diseases.[4] Systematic investigations of curcumin revealed a wide spectrum of beneficial properties including antioxidant, anti-inflammatory, antimicrobial, and anticancer activities.[5] In addition, it was shown to protect neurons against β-amyloid peptide toxicity and to bind to β-amyloid plaques of transgenic mouse models of Alzheimer's disease.[6] In view

*To whom correspondence should be addressed. Telephone: +30210 6503555. Fax: +30210 6511767. E-mail: pelmar@bio.demokritos.gr.

(1) Sagnou, M.; Tsoukalas, C.; Triantis, C.; Raptopoulou, C. P.; Terzis, A.; Pirmettis, I.; Pelecanou, M.; Papadopoulos, M. *Inorg. Chim. Acta* **2010**, *363*, 1649–1653.

(2) Benny, P. D.; Fugate, G. A.; Barden, A. O.; Morley, J. E.; Silva-Lopez, E.; Twamley, B. *Inorg. Chem.* **2008**, *47*, 2240–2242.

(3) Govindarajan, V. S.; Stahl, W. H. *Crit. Rev. Food Sci. Nutr.* **1980**, *12*, 199–301.

(4) Hatcher, H.; Planalp, R.; Cho, J.; Torti, F. M.; Torti, S. V. *Cell. Mol. Life Sci.* **2008**, *65*, 1631–1652.

(5) (a) Anand, P.; Thomas, S. G.; Kunnumakkara, A. B.; Sundaram, C.; Harikumar, K. B.; Sung, B.; Tharakan, S. T.; Misra, K.; Priyadarsini, I. K.; Rajasekharan, K. N.; Aggarwal, B. B. *Biochem. Pharmacol.* **2008**, *76*, 1590–1611. (b) Aggarwal, B. B.; Sundaram, C.; Malani, N.; Ichikawa, H. *Adv. Exp. Med. Biol.* **2007**, *595*, 1–75.

(6) (a) Yang, F.; Lim, P. L. G. P.; Begum, A. N.; Ubeda, O. J.; Simmons, M. R.; Ambegaokar, S. S.; Chen, P.; Kayed, R.; Glabe, C. G.; Frautschy, S. A.; Cole, G. M. *J. Biol. Chem.* **2005**, *280*, 5892–5901. (b) Garcia-Alloza, M.; Borrelli, L. A.; Rozkalne, A.; Hyman, B. T.; Bacskai, B. J. *J. Neurochem.* **2007**, *102*, 1095–1104.

Published on Web 01/21/2011

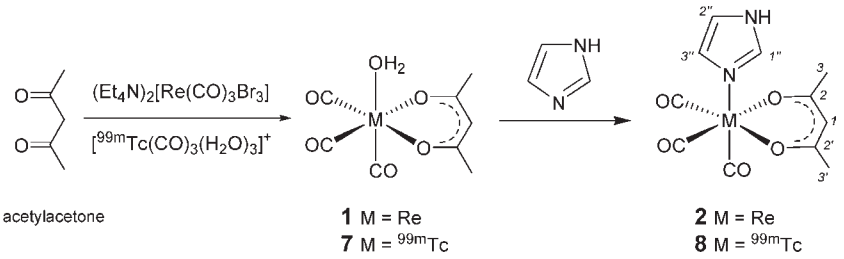

Figure 1. Synthetic scheme leading to complex **2** and its ^{99m}Tc-analogue **8**.

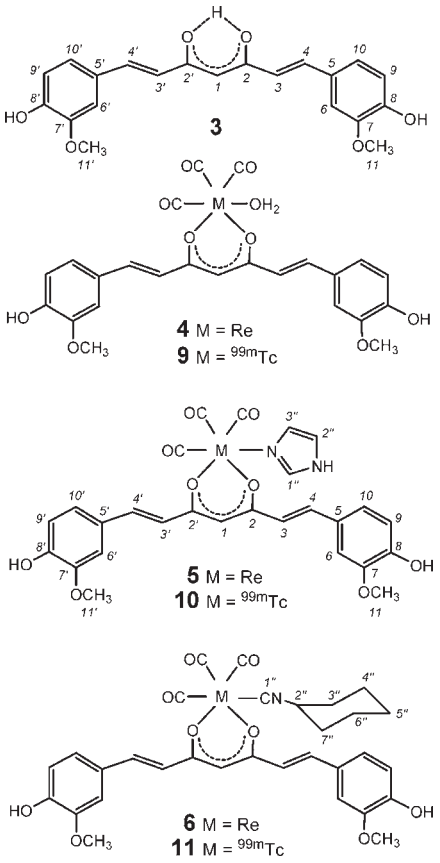

Figure 2. Structure of curcumin (**3**) and its complexes with the $[M(CO)_3]^+$ core.

of the wide range of pharmacologic activity of curcumin, the preparation of its complex with ^{99m}Tc, the most commonly used radionuclide in nuclear medicine,[7] will serve as a probe for the application of this outstanding molecule to the field of radiodiagnosis of a wide spectrum of diseases. Furthermore, through the analogous ^{186}Re/^{188}Re complexes,[8] applications to tumor radiotherapy may be worth investigating. Complexes of curcumin with transition metal ions, such as Fe(III), Fe(II), Pd(II), Cu(II), Hg(II), VO(IV), and so forth, have been reported in the literature[9,10] with a variety of coligands. Complexation of curcumin with Re and ^{99m}Tc appeared recently in a specialized technetium symposium,[11] and to our knowledge this is the first time that "2 + 1" complexes of curcumin appear in the literature as a full paper.

Experimental Section

Materials and Methods. All reagents and organic solvents used in this study were purchased from Aldrich and used without further purification. Curcumin (95% total curcuminoid content) was purchased from Alfa Aesar.

Solvents for high-performance liquid chromatography (HPLC) were HPLC-grade. They were filtered through membrane filters (0.22 μm, Millipore, Milford, MA) and degassed by a helium flux before and during use. $[NEt_4]_2[Re(CO)_3Br_3]$ was prepared according to a published procedure.[12] For ^{99m}Tc labeling, a kit containing 5.5 mg of $NaBH_4$, 4 mg of Na_2CO_3, and 10 mg of Na−K tartrate was purged with CO gas prior to addition of $Na^{99m}TcO_4$, as described in the literature.[13]

IR spectra were recorded on a Nicolet 6700 ATR-IR from Thermo Scientific. Mass spectra were recorded on an ESI Navigator Finnigan spectrometer. NMR spectra were acquired at 25 °C in DMSO-d_6 on a 500 MHz Bruker DRX-Avance spectrometer, using two-dimensional ^{1}H−^{1}H (COSY, NOESY) and ^{1}H−^{13}C (HSQC, HMBC) correlation techniques. Tetramethylsilane (TMS) was used as the internal reference. Elemental analysis for C, H, and N was performed on a Perkin-Elmer 2400 automatic elemental analyzer. HPLC analysis was performed on a Waters 600 chromatography system coupled to both a Waters 2487 Dual λ Absorbance detector and a Gabi gamma detector from Raytest. Separations were achieved on a C-18 reverse phase column (25.4 cm × 0.4 cm, 5 μm porosity) eluted with a binary gradient system at a 1 mL/min flow rate. Mobile phase A was methanol containing 0.1% trifluoroacetic acid, while mobile phase B was water containing 0.1% trifluoroacetic acid. The elution gradient was 0−1 min 100% B (0% A), followed by a linear gradient to 80% A (20% B) in 8 min; this composition was held for another 15 min. After a column wash with 95% A for 5 min, the column was re-equilibrated by applying the initial conditions (100% B) for 15 min prior to the next injection.

(7) Jurisson, S. S.; Lydon, J. D. *Chem. Rev.* **1999**, *99*, 2205–2218.
(8) Hashimoto, K.; Yoshihara, K. *Top. Curr. Chem.* **1996**, *176*, 275–291.
(9) (a) Kuhlwein, F.; Polborn, K.; Beck, W. *Z. Anorg. Allg. Chem.* **1997**, *623*, 1211–1219. (b) Valentini, A.; Conforti, F.; Crispini, A.; De Martino, A.; Condello, R.; Stellitano, C.; Rotilio, G.; Ghedini, M.; Federici, G.; Bernardini, S.; Pucci, D. *J. Med. Chem.* **2009**, *52*, 484–491. (c) Waranyoupalin, R.; Wongnawa, S.; Wongnawa, M.; Pakawatchai, C.; Panichayupakaranant, P.; Sherdshoopongse, P. *Cent. Eur. J. Chem.* **2009**, *7*, 388–394. (d) Modi, G.; Pitre, K. S. *J. Coord. Chem.* **2009**, *62*, 931–939. (e) Zebib, B.; Mouloungui, Z.; Noirot, V. *Bioorg. Chem. Appl.* **2010**, 1–8. (f) Borsari, M.; Ferrari, E.; Grandi, R.; Saladini, M. *Inorg. Chim. Acta* **2002**, *328*, 61–68.
(10) (a) John, V. D.; Krishnankutty, K. *Transition Met. Chem.* **2005**, *30*, 229–233. (b) Mohammadi, K.; Thompson, K. H.; Patrick, B. O.; Storr, T.; Martins, C.; Polishchuk, E.; Yuen, V. G.; McNeill, J. H.; Orvig, C. *J. Inorg. Biochem.* **2005**, *99*, 2217–2225. (c) Song, Y.-M.; Xu, J.-P.; Ding, L; Hou, Q.; Liu, J.-W.; Zhu, Z.-L. *J. Inorg. Biochem.* **2009**, *103*, 396–400.
(11) (a) Pignedoli, F.; Zobi, F.; Saladini, M.; Alberto, R. *Technetium and Other Radiometals in Chemistry and Medicine*; Servici Grafici Editoriali: Padova, 2010; p 99. (b) Sagnou, M.; Benaki, D.; Paravatou-Petsotas, M.; Pirmettis, I.; Papadopoulos, M.; Pelecanou, M. *Technetium and Other Radiometals in Chemistry and Medicine*; Servici Grafici Editoriali: Padova, 2010; p. 109
(12) Alberto, R.; Schibli, R.; Egli, A.; Schubiger, P. A. *J. Am. Chem. Soc.* **1998**, *120*, 7987–7988.
(13) Alberto, R.; Egli, A.; Abram, U.; Hegetschweiler, K.; Gramlich, V.; Schubiger, P. A. *J. Chem. Soc., Dalton Trans.* **1994**, 2815–2820.

Table 1. ^{1}H Chemical Shifts (δ, ppm) for Complexes **2**, **5**, **6**, and **4** as well as for the Prototype Compound Curcumin (**3**) in DMSO-d_6 at 25 °C[a]

	2	**5**	**6**	**4**[b]	**3** (curcumin)[c,d]
H-1	5.47	5.87	5.96	6.02	6.05
H-3, H-3′	1.91	6.68, $^3J_{trans}$ = 15.7 Hz	6.74, $^3J_{trans}$ = 15.7 Hz	6.76, $^3J_{trans}$ = 15.7 Hz	6.74, $^3J_{trans}$ = 15.9 Hz
H-4, H-4′		7.38, $^3J_{trans}$ = 15.7 Hz	7.36, $^3J_{trans}$ = 15.7 Hz	7.41	7.53, $^3J_{trans}$ = 15.9 Hz
H-6, H-6′		7.28, J_{meta} = 1.4 Hz	7.29, J_{meta} = 1.2 Hz	7.30	7.31
H-9, H-9′		6.78, J_{ortho} = 8.2 Hz	6.79, J_{ortho} = 8.3 Hz	6.80	6.81, J_{ortho} = 8.0 Hz
H-10, H-10′		7.12, J_{ortho} = 8.2 Hz, J_{meta} = 1.4 Hz	7.13, J_{ortho} = 8.3 Hz, J_{meta} = 1.2 Hz	7.14	7.14, J_{ortho} = 8.0 Hz
H-11, H-11′		3.82	3.83	3.83	3.83
OH		9.7 (broad)	9.5 (broad)	9.5 (broad)	9.7 (broad)
H-1″	7.87	7.87			
H-2″	7.26	7.23	4.22		
H-3″	6.88	6.91	1.69, 1.64		
H-4″			1.46, 1.35		
H-5″			1.32, 1.26		
H-6″			1.46, 1.35		
H-7″			1.69, 1.64		
NH	12.9 (broad)	12.8 (broad)			

[a] The numbering of the atoms is shown in Figures 1 and 2. [b] In DMSO-d_6, the exchange of the labile water ligand with DMSO-d_6 is highly probable. [c] The enolic proton of curcumin appearing according to the literature at ~16 ppm was not visible in our spectra, apparently due to exchange with the water present in DMSO-d_6. [d] J_{meta} was not measurable for the phenyl protons of curcumin.

***fac*-Re(CO)$_3$(acac)(imi) 2.** Complex **2** was synthesized through the intermediate formation of the *fac*-Re(CO)$_3$(acac)(H$_2$O) **1** according to published procedures[1,2] with slight modifications. Briefly, to the solution of acetylacetone (100 mg, 1.0 mmol) in water (8 mL, pH 6, adjusted with addition of small aliquots of a 0.1 N sodium bicarbonate solution), the rhenium precursor, [NEt$_4$]$_2$[Re(CO)$_3$Br$_3$] (456 mg, 0.6 mmol), was added. The solution was heated to 85 °C for 4 h to yield **1** as a yellowish precipitate that was filtered and washed with water. Yield: 60%. HPLC: t_R = 14.7 min.

To a stirred solution of **1** (39 mg, 0.1 mmol) in methanol (10 mL), a solution of imidazole (6.8 mg, 0.1 mmol) in methanol (2 mL) was added. The solution was stirred under reflux for 3 h and the reaction progress was monitored by HPLC. Subsequently, the solvent was removed under reduced pressure and the residue was recrystallized from methanol/water to give complex **2** as a yellowish solid. Yield: 92%. Slow evaporation of a methanol/water solution afforded crystals suitable for X-ray analysis. HPLC: t_R = 14.9 min, IR (cm^{-1}): 2009, 1867, 1579, and 1519; Anal. Calcd (%) for C$_{11}$H$_{11}$N$_2$O$_5$Re: C, 30.20; H, 2.53; N, 6.40. Found: C, 30.29; H, 2.75; N, 6.63%. ^{1}H and ^{13}C NMR data are given in Tables 1 and 2.

***fac*-Re(CO)$_3$(curcu)(H$_2$O) 4.** For the preparation of **4**, to a solution of curcumin (36.8 mg, 0.1 mmol) in methanol (3 mL) and acetate buffer pH 5 (1.5 mL), a solution of [NEt$_4$]$_2$-[Re(CO)$_3$Br$_3$] precursor (77 mg, 0.1 mmol) in methanol (1.5 mL) was added. The cloudy mixture was heated at 60 °C until a clear orange-red solution was formed. The solvent was removed under reduced pressure, and the remaining solid was purified by column chromatography (silica gel, CHCl$_3$/CH$_3$OH, 98:2) to give complex **4** as a red-brown solid. Yield: 70%. HPLC: t_R = 15.5 min. IR (cm^{-1}): 2013, 1872, 1624, 1591. Anal. Calcd (%) for C$_{24}$H$_{21}$O$_{10}$Re: C, 43.97; H, 3.23. Found: C, 44.28; H, 3.59%. ^{1}H and ^{13}C NMR data are given in Tables 1 and 2. MS (ESI): m/z (M + H)$^+$ 678.2 and 680.2 (calculated for C$_{26}$H$_{22}$NO$_9$^{185}Re and C$_{26}$H$_{22}$NO$_9$^{187}Re, 678.090 and 680.093 corresponding to the complex with CH$_3$CN in the place of water).

***fac*-Re(CO)$_3$(curcu)(imi) 5.** To a stirred solution of **4** (65.5 mg, 0.1 mmol) in methanol (10 mL), a solution of imidazole (6.8 mg, 0.1 mmol) in methanol (2 mL) was added. The solution was stirred with moderate heating at 50 °C for 2 h, and the reaction progress was monitored by HPLC. Subsequently, the solvent was removed under reduced pressure and the residue was recrystallized from methanol/water to give complex **5** as an orange-red solid. Yield: 88%. HPLC: t_R = 15.7 min. IR (cm^{-1}): 2011, 1862 (broad), 1618, 1590. Anal. Calcd (%) for C$_{27}$H$_{23}$N$_2$O$_9$Re: C, 45.95; H, 3.29; N, 3.97. Found: C, 46.09; H, 3.55; N, 3.63%. MS (ESI): m/z (M + H)$^+$ 705.4 and 707.4 (calculated for C$_{27}$H$_{23}$N$_2$O$_9$^{185}Re and C$_{27}$H$_{23}$N$_2$O$_9$^{187}Re, 705.463 and 707.446). ^{1}H and ^{13}C NMR data are given in Tables 1 and 2.

***fac*-Re(CO)$_3$(curcu)(isc) 6.** Complex **6** was synthesized in a similar fashion to complex **5** using isocyanocyclohexane (11 mg, 0.1 mmol) as the monodentate ligand, but without heating. The product of the reaction was purified by column chromatography (silica gel, CHCl$_3$/CH$_3$OH 98:2) to give complex **6** as a red-brown solid. Yield: 81%. HPLC: t_R = 17.5 min. IR (cm^{-1}): 2194, 2014, 1923, 1881, 1622, 1589. Anal. Calcd (%) for C$_{31}$H$_{30}$NO$_9$Re: C, 49.86; H, 4.05; N, 1.88. Found: C, 49.67; H, 3.88; N, 1.65. MS (ESI): m/z (M + H)$^+$ 746.4 and 748.4 (calculated for C$_{31}$H$_{30}$NO$_9$^{185}Re and C$_{31}$H$_{30}$NO$_9$^{187}Re, 746.539 and 748.542). ^{1}H and ^{13}C NMR data are given in Tables 1 and 2.

X-ray Structure Determination of Complex 2. A crystal of complex **2** with approximate dimensions 0.77 × 0.30 × 0.11 mm^3 was taken from the mother liquor and immediately cooled to −93 °C. Diffraction measurements were made on a Rigaku R-AXIS SPIDER Image Plate diffractometer using graphite monochromated Mo Kα radiation. Data collection (ω-scans) and processing (cell refinement, data reduction, and empirical absorption correction) were performed using the CrystalClear program package.[14] The structure was solved by direct methods using SHELXS-97[15] and refined by full-matrix least-squares techniques on F^2 with SHELXL-97.[16] Important crystallographic data are listed in Table 3. Further experimental crystallographic details for **2**: $2\theta_{max}$ = 52°; reflections collected/unique/used, 11 619/2729 [R_{int} = 0.0326]/2729; 174 parameters refined; $(\Delta/\sigma)_{max}$ = 0.001; $(\Delta\rho)_{max}/(\Delta\rho)_{min}$ = 1.067/−2.042 e/Å^3; $R1/wR2$ (for all data), 0.0316/0.0662. All hydrogen atoms were introduced at calculated positions as riding on bonded atoms. All non-hydrogen atoms were refined anisotropically.

^{99m}Tc Complex 8. Complex **8** was synthesized through the intermediate formation of the *fac*-^{99m}Tc(CO)$_3$(acac)(H$_2$O) complex **7**, as previously described.[1] Briefly, a freshly prepared solution of the *fac*-[^{99m}Tc(CO)$_3$(H$_2$O)$_3$]$^+$ precursor (pH 6) (400 μL) was added to a vial containing a solution of acetylacetone (1 mg) in water (600 μL). The vial was sealed, flushed with N$_2$, and heated for 15 min at 70 °C. HPLC analysis demonstrated the

(14) Rigaku/MSC. *CrystalClear*; Rigaku/MSC Inc.: The Woodlands, Texas, 2005.

(15) Sheldrick, G. M. *SHELXS-97, Structure Solving Program*; University of Göttingen: Germany, 1997.

(16) Sheldrick, G. M. *SHELXL-97, Crystal Structure Refinement Program*; University of Göttingen: Germany, 1997.

Table 2. ^{13}C Chemical Shifts (δ, ppm) for Complexes **2**, **5**, **6**, and **4** as well as for the Prototype Compound Curcumin (**3**) in DMSO-d_6 at 25 °C[a]

	2	5	6	4[b]	3 (curcumin)
C-1	101.82	104.00	104.06	103.85	100.84
C-2, C-2′	187.83	178.87	180.09	179.28	183.20
C-3, C-3′	27.19	124.71	124.59	124.24	121.08
C-4, C-4′		138.73	139.01	138.86	140.72
C-5, C-5′		126.40	126.76	127.00	126.31
C-6, C-6′		111.16	111.26	110.93	111.35
C-7, C-7′		148.06	147.95	147.70	148.04
C-8, C-8′		149.36	148.77	148.75	149.47
C-9, C-9′		115.77	115.71	115.31	115.74
C-10, C-10′		122.35	122.26	122.12	123.17
C-11, C-11′		55.59	55.67	55.29	55.73
C-1″	138.02	139.02	141.39		
C-2″	118.23	119.79	53.65		
C-3″	127.42	126.96	30.88		
C-4″			21.04		
C-5″			24.17		
C-6″			21.04		
C-7″			30.88		
C≡O	198.34, 199.46	200.57, 199.04	194.89, 194.41		

[a] The numbering of the atoms is shown in Figures 1 and 2. [b] In DMSO-d_6, the exchange of the labile water ligand with DMSO-d_6 is highly probable.

formation of a single complex (t_R = 15.0 min, radiochemical yield > 90%) assigned to the *fac*-^{99m}Tc(CO)$_3$(acac)(H$_2$O) complex **7** by comparative HPLC analysis using a sample of the *fac*-Re(CO)$_3$(acac)(H$_2$O) complex **1** as reference. To the solution of **7**, imidazole (1 mg) was added, and the mixture was heated at 80 °C for 30 min. HPLC analysis of the reaction mixture showed in addition to the peak of **7** the presence of a second radioactive peak (t_R = 15.3 min, radiochemical yield = 35−45%), that was assigned to **8** by comparative HPLC studies using a sample of the well-characterized *fac*-Re(CO)$_3$(acac)(imi) complex **2** as reference.

^{99m}Tc Complex 9. For the synthesis of **9**, essentially the same procedure was followed as the one described above for **7**, except that curcumin (1.3 mg) was dissolved in DMSO (400 μL). After cooling, HPLC analysis demonstrated the formation of a single complex (t_R = 15.9 min, radiochemical yield > 90%) which was assigned to the *fac*-^{99m}Tc(CO)$_3$(curcu)(H$_2$O) complex **9** by comparative HPLC analysis using the well-characterized Re complex **4** as reference (Figure 3A, B).

^{99m}Tc Complex 10. For the synthesis of **10**, imidazole (1 mg) was added to a solution of **9** (400 μL) and the reaction mixture was heated for 30 min at 70 °C. HPLC analysis of the reaction mixture showed the presence of a radioactive peak (t_R = 16.3 min, radiochemical yield 25−35%), corresponding to **10** by comparison of its HPLC retention time to the well-characterized *fac*-Re(CO)$_3$(curcu)(imi) complex **5**.

^{99m}Tc Complex 11. For the synthesis of complex **11**, isocyanocyclohexane (1 mg) was added to a solution of **9** (400 μL) and the mixture was left at room temperature for 30 min. HPLC analysis of the reaction mixture demonstrated the formation of one main radioactive peak (t_R = 17.9 min, radiochemical yield > 90%) corresponding to **11** by comparative HPLC analysis using a sample of the well-characterized Re analogue **6** as reference (Figure 3C, D).

All ^{99m}Tc complexes were stable for a period of at least 2 half-lives at room temperature in their preparation reaction mixtures (aqueous medium, pH 6) as witnessed by HPLC. For all ^{99m}Tc preparations, the radioactivity recovery of the HPLC column after the injections was monitored and found to be quantitative.

***β*-Amyloid Plaque Staining.** Five micrometer thick serial sections of fixed and paraffin-embedded neuropathologically diagnosed AD brain were deparaffinized with 2 × 5 min washes in xylene; 2 × 3 min washes in 100% ethanol; 5 min washes in 80% ethanol/H$_2$O; 5 min washes in 60% ethanol/H$_2$O; running tap water for 10 min, and then incubated in PBS (1.3 M NaCl, 27 mM KCl, 81 mM Na$_2$HPO$_4$, 14.7 mM KH$_2$PO$_4$, pH 7) for 15 min. The tissue preparations were treated with 40 μM solutions of curcumin and curcumin complexes in DMSO (prepared from 4 mM stock solutions in DMSO) for 45 min. The sections were finally washed with 40% ethanol for 1 min, followed by rinsing with water for 30 s. Fluorescent observation was performed with a Zeiss Axioplan2 microscope equipped with a FITC filter set (excitation at 495 nm).

Table 3. Crystallographic Data for Complex **2**

complex **2**	
formula	$C_{11}H_{11}N_2O_5Re$
Fw	437.42
space group	*Pbca*
a (Å)	13.5512(3)
b (Å)	13.6051(2)
c (Å)	15.1648(3)
α (°)	90
β (°)	90
γ (°)	90
V (Å^3)	2795.87(9)
Z	8
T (°C)	180
radiation	Mo Kα (0.71073 Å)
ρ_{calcd} (g cm^{-3})	2.078
μ (mm^{-1})	8.709
reflections with $I > 2\sigma(I)$	2419
R_1[a]	0.0270
wR_2[a]	0.0644

[a] $w = 1/[\sigma^2(F_o^2) + (\alpha P)^2 + bP]$, $P = (\max F_o^2,0) + 2F_c^2)/3$, $R_1 = \Sigma(|F_o| - |F_c|)/\Sigma(|F_o|)$, and $wR_2 = \{\Sigma[w(F_o^2 - F_c^2)^2]/\Sigma[w(F_o^2)^2]\}^{1/2}$.

Results and Discussion

Synthesis and Characterization of 2. Complex **2** was synthesized through the intermediate formation of Re(CO)$_3$(acac)(H$_2$O) **1** (Figure 1) according to published procedure[1,2] and employing imidazole as the monodentate ligand. Imidazole is a ligand of interest because of its biological significance being part of many important biomolecules, bioactive molecules, and pharmaceuticals.[17] It forms stable complexes with transition metals and has

(17) (a) Sundberg, R. J.; Martin, R. B. *Chem. Rev.* **1974**, *74*, 471–517. (b) Brown, E. G. *Ring Nitrogen and Key Biomolecules*; Kluwer Academic: Dordrecht, Netherlands,1998.

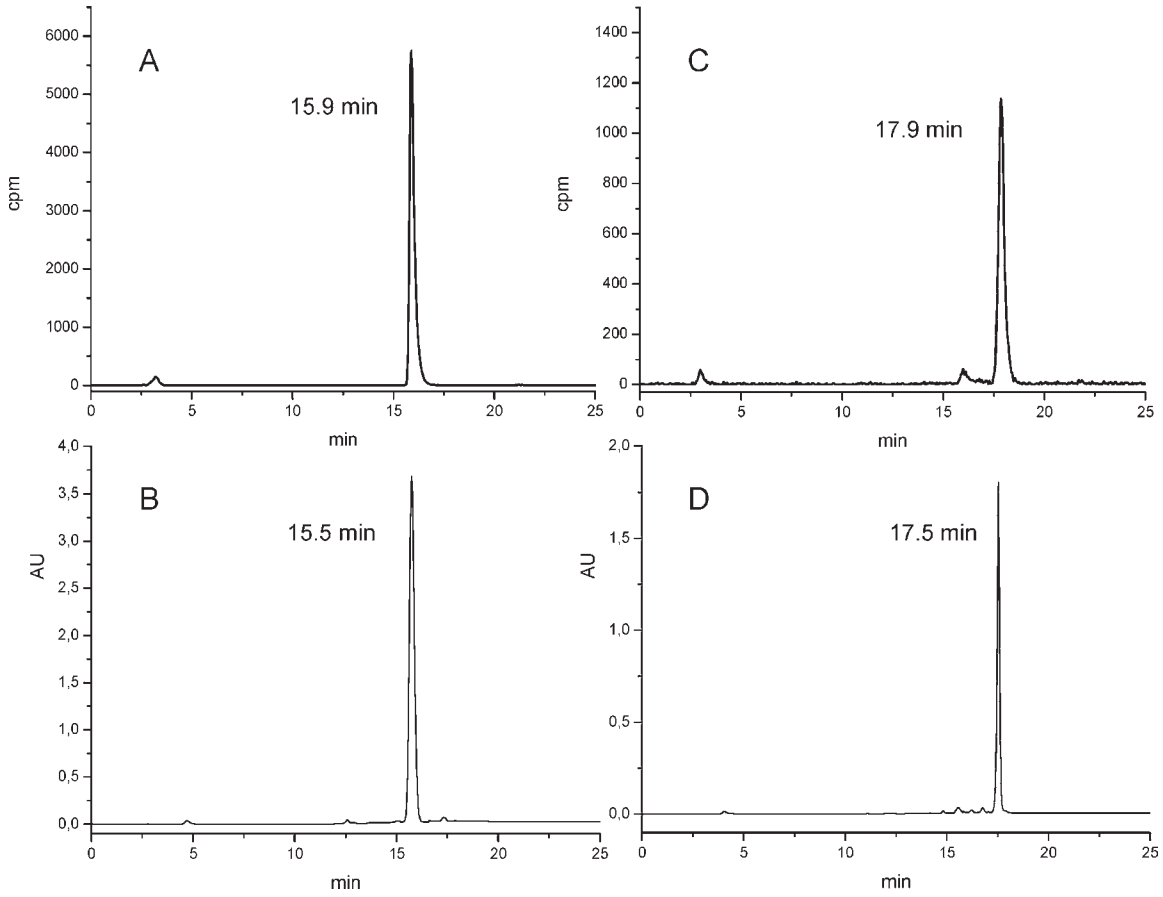

Figure 3. Comparative reverse-phase HPLC chromatograms. Radiometric detection: (A) *fac*-^{99m}Tc(CO)$_3$(curcu)(H$_2$O) **9** and (C) *fac*-^{99m}Tc(CO)$_3$(curcu)-(isc) **11**. UV detection at 254 nm: (B) *fac*-Re(CO)$_3$(curcu)(H$_2$O) **4** and (D) *fac*-Re(CO)$_3$(curcu)(isc) **6**.

already been applied as a monodentate ligand for the [M(CO)$_3$]$^+$ (M = Re, ^{99m}Tc) core.[18] Addition of imidazole in the solution of **1** led very quickly to the replacement of the water ligand to give the *fac*-Re(CO)$_3$(acac)(imi) complex **2** as a single product in excellent yield. Complex **2** was collected as a yellowish solid and characterized by elemental analysis, spectroscopic methods, and X-ray crystallography. It is stable in the solid state and in solution for months as shown by HPLC and NMR.

The infrared spectra of complex **2** show strong bands at 2009 and 1867 cm^{-1} attributed to the C≡O stretch of the *fac*-[Re(CO)$_3$]$^+$ unit.[19] The carbonyl peaks of the enolic form of acetylacetone at 1605 cm^{-1} are decreased in intensity and shifted to lower energy appearing at 1579 and 1519 cm^{-1}, a shift that is also present in the IR spectrum of the analogous *fac*-Re(CO)$_3$(acac)(isc)[1] complex.

^{1}H and ^{13}C NMR chemical shifts for complex **2** in DMSO-d_6 are given in Tables 1 and 2, and the numbering of the atoms is shown in Figure 1. In the NMR spectra of complex **2** integration of the peaks shows that the acetylacetone and imidazole moieties are present in a 1:1 ratio. The chemical shifts of the acetylacetone moiety are very similar (≤0.1 ppm for the ^{1}H and ≤0.5 ppm for the ^{13}C) to those reported for the analogous *fac*-Re(CO)$_3$-(acac)(isc)[1] and *fac*-Re(CO)$_3$(acac)(pyr)[2] in which acetylacetone coordinates to Re(I) through the acetylacetonate anion. This fact indicates that, also in the case of **2**, similar coordination takes place with formation of the six-membered chelate ring with enolate type resonance typical of β-diketones.[20]

In the ^{1}H spectra of complex **2** (and the related *fac*-Re(CO)$_3$(acac)(isc)[1] and *fac*-Re(CO)$_3$(acac)(pyr)[2] complexes), small upfield shifts are noted (within 0.15 ppm) for the acetylacetone moiety upon coordination to the [Fe(CO)$_3$]$^+$ core. This is in agreement with a number of studies on complexes of the enolate form of β-diketones[21] with a variety of divalent and trivalent ions that report small or nonexistent chemical shift changes upon coordination. In the ^{13}C spectra of complex **2** (and the related *fac*-Re(CO)$_3$(acac)(isc)[1] and *fac*-Re(CO)$_3$(acac)(pyr)[2] complexes), it is interesting to note that while the C-1 and C-3(C-3′) carbons shift downfield by approximately 1.5 and 2.5 ppm, respectively, compared to plain acetylacetone,[22] the C-2(C-2′) carbonyl carbons are shifted upfield by approximately 2.5 ppm, apparently reflecting an increase in π-electron density at the carbonyl carbons in this type of complexes.

(18) (a) Kromer, L.; Spingler, B.; Alberto, R. *Dalton Trans.* **2008**, 5800–5806. (b) Mundwiler, S.; Kündig, M.; Ortner, K.; Alberto, R. *Dalton Trans.* **2004**, 1320–1328.

(19) Alves, S.; Paulo, A.; Correia, J. D. G.; Domingos, A.; Santos, I. *J. Chem. Soc., Dalton Trans.* **2002**, 4714–4719. (b) Vitor, A.; Alves, S.; Correia, J. D. G.; Paulo, A.; Santos, I. *J. Organomet. Chem.* **2004**, *689*, 4764–4774.

(20) Holm, R. H.; Cotton, F. A. *J. Am. Chem. Soc.* **1958**, *80*, 5658–5663.

(21) (a) Smith, J. A. S.; Thwaites, J. D. *Discuss. Faraday Soc.* **1962**, *34*, 143–146. (b) Carty, A. J.; Tuck, D. J.; Bullock, E. *Can. J. Chem.* **1965**, *43*, 2559–2565.

(22) Claramunt, R. M.; López, C.; Lott, S.; Santa María, M. D.; Alkorta, I.; Elguero, J. *Helv. Chim. Acta* **2005**, *88*, 1931–1942.

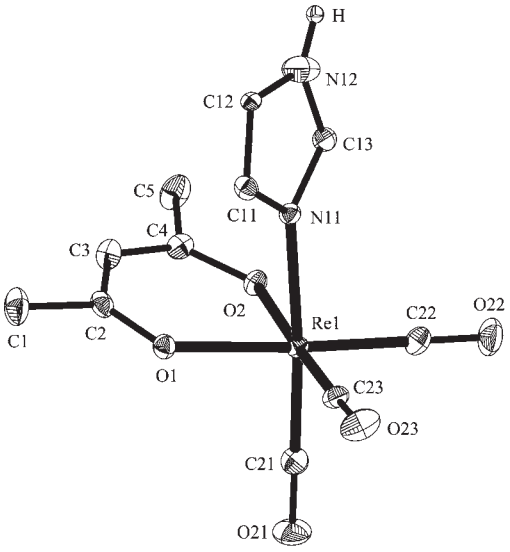

Figure 4. Labeled plot of the structure of **2** with ellipsoids drawn at the 30% probability level. Hydrogen atoms (except that of the imidazole nitrogen) have been omitted for clarity.

For the imidazole coligand, upon coordination downfield shifts of approximately 0.2 and 3 ppm are noted for H-1″ and C-1″, respectively, relative to their values in free imidazole in the same solvent (our data, Figure S1, Supporting Information), while the previously equivalent H-2″, H-3″, C-2″, and C-3″ are magnetically differentiated. H-3″ was distinguished from H-2″ based on the presence of an NOE peak (Figure S2, Supporting Information) with the methyl H-3(H-3′) protons of the acetylacetone moiety. It is interesting to note that coordination of imidazole has an inverse effect on the shifts of atoms at position 2″ (downfield for H-2″, upfield for C-2″) and position 3″ (upfield for H-3″, downfield for C-3″) relative to their shifts in free imidazole, a fact that possibly indicates the existence of local magnetic anisotropy regions generated by the resonating acetylacetonate moiety or even the C≡O coligands.

Description of the Crystal Structure of Complex 2. The molecular structure of **2** is given in Figure 4, and selected bond distances and angles are listed in Table 4. The coordination geometry about rhenium in **2** is distorted octahedral comprised by the OO bidentate chelator, acetylacetonate, the nitrogen atom of the imidazole ring, and the three carbonyl groups. The apical positions of the octahedron are occupied by the imidazole nitrogen atom and one of the carbonyl groups. Rhenium almost lies (∼0.07 Å) in the equatorial plane in **2**. The six-membered ring in the coordination sphere, defined by the O−C−C−C−O chelating atoms of acetylacetonate and the metal ion, is almost planar with the largest displacement for C3 being 0.16 Å. The angles around the metal within the tetragonal plane of the octahedron range from 85.7(1) to 93.7(2)°, whereas those involving the apical atoms range from 80.9(1) to 95.5(2)°. All bond distances in the coordination sphere fall in the ranges observed in analogous complexes. In the lattice structure, the presence of weak N−H···O intermolecular interactions links the molecules of **2** into one-dimensional assemblies which extend parallel to the crystallographic *c*-axis (N12···O1 (x, 0.5 − y, 0.5 + z) = 3.311 Å, H12N···O1 = 2.561 Å, N12−H12N···O1 = 143.6°).

Table 4. Selected Interatomic Distances (Å) and Angles (deg) in Complex **2**

distances (Å)			
Re(1)−C(21)	1.901(5)	Re(1)−O(1)	2.128(3)
Re(1)−C(22)	1.907(5)	Re(1)−O(2)	2.129(3)
Re(1)−C(23)	1.912(5)	Re(1)−N(11)	2.187(4)
angles (deg)			
C(21)−Re(1)−C(22)	88.3(2)	C(23)−Re(1)−O(2)	175.9(2)
C(21)−Re(1)−C(23)	89.0(2)	O(1)−Re(1)−O(2)	85.7(1)
C(22)−Re(1)−C(23)	87.0(2)	C(21)−Re(1)−N(11)	174.6(2)
C(21)−Re(1)−O(1)	94.9(2)	C(22)−Re(1)−N(11)	95.5(2)
C(22)−Re(1)−O(1)	176.7(2)	C(23)−Re(1)−N(11)	95.1(2)
C(23)−Re(1)−O(1)	93.7(2)	O(1)−Re(1)−N(11)	81.3(1)
C(21)−Re(1)−O(2)	95.1(2)	O(2)−Re(1)−N(11)	80.9(1)
C(22)−Re(1)−O(2)	93.3(2)		

Synthesis and Characterization of Curcumin Complexes 5, 6 and of the Intermediate Complex 4. For the synthesis of the curcumin complexes, essentially the same procedure was employed as the one described for complex **2**. Formation of the curcumin complexes proceeded through the intermediate formation of the aqua complex **4** which was isolated as a red-brown solid and subjected to analysis. Addition of equimolar quantities of imidazole in methanolic solution of **4** led to the formation of complex **5**, while addition of equimolar quantities of isocyanocyclohexane led to the formation of complex **6**. Both **5** and **6** were obtained in high yield and were characterized by elemental analysis, mass spectrometry, and NMR and IR spectroscopies. All attempts to isolate a crystal suitable for X-ray analysis were not successful.

The ESI spectra of complexes **5**, **6** and of the intermediate complex **4** gave $(M + H)^+$ peaks at m/z values corresponding to the structures of Figure 2. Specifically, complex **5** gave peaks at m/z 705.4 and 707.4 corresponding to the calculated $(M + H)^+$ values for $C_{27}H_{23}N_2O_9{}^{185}Re$ (705.463) and $C_{27}H_{23}N_2O_9{}^{187}Re$ (707.466), and complex **6** gave peaks at m/z 746.4 and 748.4 corresponding to the calculated $(M + H)^+$ values for $C_{31}H_{30}NO_9{}^{185}Re$ (746.539) and $C_{31}H_{30}NO_9{}^{187}Re$ (748.542), respectively. The m/z peaks obtained from the analysis of complex **4** at 678.2 and 680.2 correspond to the complex bearing an acetonitrile in the place of water (theoretically calculated $(M + H)^+$ peaks for the $C_{26}H_{22}NO_9{}^{185}Re$ and $C_{26}H_{22}NO_9{}^{18}Re$ complexes bearing a CH_3CN as monodentate ligand are at m/z 678.090 and 680.093), a fact that can be explained by the replacement of the labile water ligand by acetonitrile that is present in the carrier solvent (CH_3CN/H_2O 50:50) of the mass spectrometer. In all cases, the percent ratio of the intensities of $^{185}Re/^{187}Re$ complex peaks corresponds to the theoretical ratio of 59.74% based on the relative $^{185}Re/^{187}Re$ abundance. Overall, the mass analysis indicates the complexation of the $Re(CO)_3{}^+$ core with curcumin in a 1:1 ratio and is in agreement with the structures of Figure 2.

The ^1H and ^{13}C NMR data for complexes **5**, **6** and for the intermediate complex **4** are presented in Tables 1 and 2, respectively. The HSQC spectrum of complex **5** and the NOESY spectrum of complex **6** are given in Figures 5 and 6, respectively, while the ^1H spectrum of complex **4** is presented in Figure S3 of the Supporting Information.

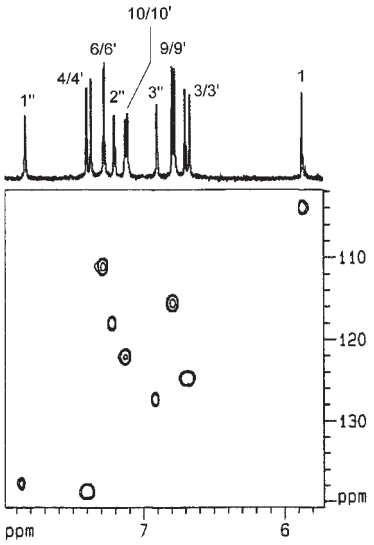

Figure 5. HSQC spectrum (range δ_H 7.98−5.72, range δ_C 140.75−101.78) of complex **5** in DMSO-d_6 at 25 °C. The numbering of the atoms is shown in Figure 2.

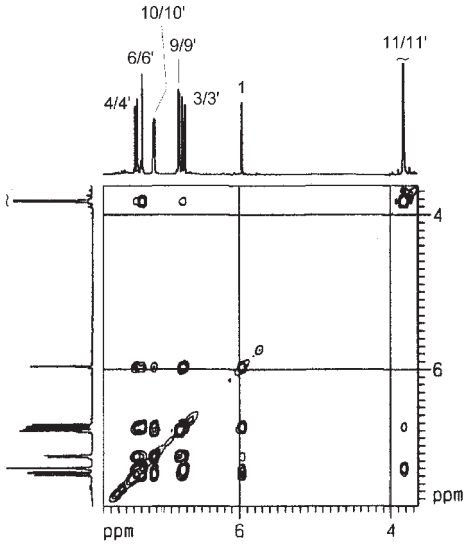

Figure 6. NOESY spectrum (range δ_H7.80−3.64 in both dimensions) of complex **6** in DMSO-d_6 at 25 °C. The numbering of the atoms is shown in Figure 2.

The chemical shifts of curcumin (**3**) that provided the basis for the structural elucidation of the complexes are also included in Tables 1 and 2 for comparison purposes and are in complete agreement with values reported in the literature.[23,24] Curcumin is a β-diketone, and a combination of spectroscopic[23−25] and crystallographic evidence[26] as well as theoretical calculations[23,27] indicate that it exists in the keto−enol tautomeric form with the enolic hydrogen equally shared by the two oxygen atoms. The NMR spectra of curcumin in solution show one set of signals corresponding to the average of all possible keto−enol structures in fast equilibrium, as a consequence of the free rotation around the single bond connecting the aromatic ring with the dienic structure.[23] The C-1 bridging carbon of curcumin in DMSO-d_6 appears at 100.8 ppm in agreement with sp^2 hybridization, and, in accordance, the H-1 proton appears as a singlet at 6.06 ppm. The C-2 and C-2′ carbonyl carbons appear at 183.2 ppm, a value lying between the theoretically calculated values for the ketonic (187.9 ppm) and enolic (174.0 ppm) carbons of curcumin.[28]

In the ^{1}H spectra of complexes **5** and **6**, peaks corresponding to the curcumin moiety and to the imidazole and isocyanocyclohexane moieties are present in a 1:1 ratio. The curcumin moiety still presents a single set of peaks indicating formation of a structure possessing symmetry elements. As can be seen in Table 1, the ^{1}H chemical shifts of the curcumin moiety in complexes **4**−**6** are very close to those of free curcumin. The aromatic proton peaks remain essentially unchanged, while small upfield shifts (up to 0.15 ppm) are noted for protons H-1, H-3(H-3′), and H-4(H-4′) close to the coordination site. Upfield shifts of the protons close to the coordination site are also noted in the spectra of the acetylacetone complex **2** and the related *fac*-Re(CO)$_3$(acac)(isc)[1] and *fac*-Re(CO)$_3$(acac)(pyr)[2] relative to free acetylacetone. A feature present in the NOESY spectra of complexes **5** and **6** and not in those of curcumin under the same conditions is the presence of NOE correlation peaks connecting protons H-3(H-3′) and H-4(H-4′) with the H-11(H-11′) protons of the methoxy aromatic substituent (Figure 6), indicative of the more rigid structure of the complexes. In the ^{13}C spectra of **4**−**6**, more pronounced differences are present, with downfield shifts noted for C-1 and C-3(C-3′) carbons (up to 3.2 and 3.6 ppm, respectively) and upfield shifts of up to 4.3 ppm noted for the C-2(C-2′) carbonyl carbons relative to those of free curcumin. These ^{13}C shift changes are in the same direction as those observed in complex **2** and the related complexes *fac*-Re(CO)$_3$(acac)(isc)[1] and *fac*-Re(CO)$_3$(acac)(pyr)[2] relative to free acetylacetone. Finally, the chemical shifts of the monodentate ligands imidazole (complex **5**) and isocyanocyclohexane (complex **6**) are very similar to those observed in the related complexes **2** and *fac*-Re(CO)$_3$(acac)(isc)[1] respectively, thus confirming their coordination.

Overall, the available NMR data on the curcumin complexes **5** and **6** are in agreement with coordination of curcumin through its β-diketo moiety in the keto−enolic form and formation of the expected structures shown in Figure 2. The spectra of complex **4** have all the characteristic features and chemical shift changes observed for complexes **5** and **6**, proving the coordination of curcumin to the metal. However, it should be noted that in DMSO-d_6 replacement of the labile water ligand by a DMSO-d_6 may have taken place, and the shifts reported may well belong to the complex bearing a DMSO-d_6 as monodentate ligand.

The IR spectra of the complexes (IR spectrum of complex **6** is shown in Figure S4 of the Supporting Information)

(23) Benassi, R.; Ferrari, E.; Lazzari, S.; Spagnolo, F.; Saladini, M. *J. Mol. Struct.* **2008**, *892*, 168–176.
(24) Unterhalt, B. *Z. Lebensm.-Unters. Forsch.* **1980**, *170*, 425–428.
(25) (a) Matthes, H. W. D.; Luu, B.; Ourisson, G. *Phytochemistry* **1980**, *19*, 2643–2650. (b) Payton, F.; Sandusky, P.; Alworth, W. L. *J. Nat. Prod.* **2007**, *70*, 143–146. (c) Krishnankutty, K.; John, V. D. *Synth. React. Inorg. Met.-Org. Chem.* **2003**, *33*, 343–358.
(26) (a) Tønnesen, H. H.; Karlsen, J.; Mostad, A. *Acta Chem. Scand. B* **1982**, *36*, 475–479. (b) Parimita, S. P.; Ramshankar, Y. V.; Suresh, S; Guru Row, T. N. *Acta Crystallogr.* **2007**, *E63*, o860–o862. (c) Mague, J. T.; Alworth, W. L.; Payton, F. L. *Acta Crystallogr.* **2004**, *C60*, 608–610.
(27) (a) Shen, L.; Ji, H. F. *Spectrochim. Acta, Part A* **2007**, *67*, 619–623. (b) Kong, L.; Priyadarsini, K. I.; Zhang, H.-Y. *THEOCHEM* **2004**, *684*, 111–116.
(28) Cornago, P.; Claramunt, R. M.; Bouissane, L.; Alkorta, I.; Elguero, J. *Tetrahedron* **2008**, *64*, 8089–8094.

are characterized by the presence of strong C≡O carbonyl peaks from the $Re(CO)_3^+$ core at 2011 and 1862 cm^{-1} for **5**, 2014, 1923, and 1881 cm^{-1} for **6**, and 2013 and 1872 cm^{-1} for the intermediate complex **4**. Also in complex **6**, the characteristic sharp peak of isonitrile at 2194 cm^{-1} is present. The carbonyl peaks of the enolate form of the curcumin moiety appear at 1618 and 1590 cm^{-1} in complex **5**, 1622 and 1589 cm^{-1} in complex **6**, and 1624 and 1591 cm^{-1} in complex **4**. In all cases, the lower energy peak is stronger. Compared to free curcumin, the carbonyl peaks of the complexes are shifted to lower energy by approximately 10 cm^{-1}, in agreement with coordination to Re(I). Similar carbonyl shifts to lower energy upon coordination have been reported in the literature for complexes of curcumin with various other metals.[10] Furthermore, in the spectra of the complexes, a new relatively strong band appears at approximately 455 cm^{-1} that has been attributed in the literature[10] to metal−oxygen bonding, further supporting the coordination of the enolate of curcumin to Re(I).

^{99m}Tc Chemistry. At the ^{99m}Tc level, the formation of the *fac*-$^{99m}Tc(CO)_3(acac)(H_2O)$ intermediate **7** proceeded in high yield as previously reported.[1,29] Replacement of the water ligand by imidazole resulted in formation of the *fac*-$^{99m}Tc(CO)_3(acac)(imi)$ **8** in moderate yield. Variations in the reaction conditions (heating time and temperature, ligand concentration) did not result in significant improvements of the radiochemical yield.

In the case of curcumin, the *fac*-$^{99m}Tc(CO)_3(curcu)(H_2O)$ complex **9** was formed in high radiochemical yield (>90%), demonstrating for the first time the potential of curcumin as an OO bidentate ligand for the $^{99m}Tc(CO)_3^+$ core. Replacement of the water by imidazole proceeded in low yield (25−35%), as in the case of the acetylacetone analogue **8**. However, replacement of the water of **9** by isocyanocyclohexane to generate **11** was almost quantitative, resulting in an overall yield of >90% for the synthesis of **11**. High radiochemical yield was also reported for the analogous *fac*-$^{99m}Tc(CO)_3(acac)(isc)$.[1] These results demonstrate that the isonitrile is a better monodentate ligand than imidazole for β-diketone complexes with the $^{99m}Tc(CO)_3^+$ core, as already reported in the literature[18] for other "2 + 1" ligand systems.

***β*-Amyloid Plaque Staining.** As a first step in the biological evaluation of the synthesized curcumin complexes, the determination of their binding affinity for β-amyloid plaques of Alzheimer's disease (AD) was selected, for a number of reasons. First, curcumin has demonstrated favorable brain permeability and satisfactory β-amyloid plaque binding in transgenic mice in vivo,[6] and recently an uptake of up to 0.69% ID/g was reported for iodo- and fluoro-labeled derivatives of curcumin in mice.[30] This fact, in combination with its low toxicity, attested by its use for centuries as a spice, food preservative, and herbal remedy, renders curcumin a suitable starting pharmacophore for the development of a radiodiagnostic for AD plaque imaging. In addition, the fluorescence properties of curcumin and its complexes

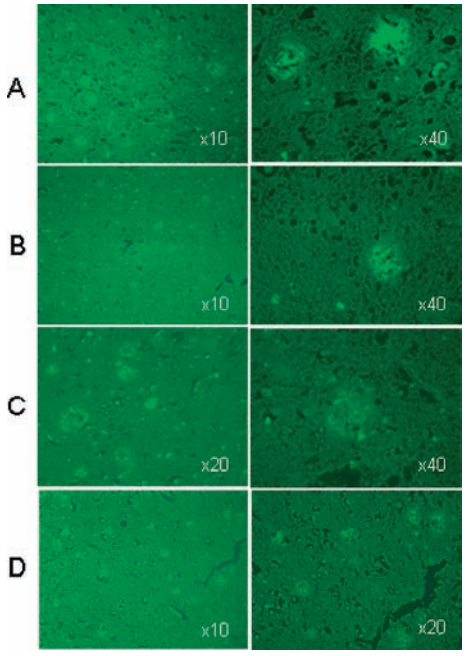

Figure 7. Fluorescence microscopy images of Alzheimer's disease brain sections stained with (A) complex **5**, (B) complex **6**, (C) complex **4**, and (D) curcumin. The magnification of the lens is indicated on each picture.

(our data, Figure S5, Supporting Information) provide a valuable tool for in vitro evaluation of binding affinities to β-amyloid plaques by fluorescence microscopy through the employment of the nonradioactive Re complexes. Finally, it should be mentioned that, despite the considerable and successful efforts in developing a PET tracer for early AD diagnosis based on β-amyloid plaque binding,[31] including the recent work on iodo- and fluoro-labeled curcumin derivatives,[30] the development of an economical and widely available ^{99m}Tc complex as a probe for AD diagnosis is still a major research target pursued by many groups worldwide.[32]

(29) Gorshkov, N. I.; Lumpov, A. A.; Miroslavov, A. E.; Suglobov, D. N. *Radiochemistry* **2005**, *47*, 45–49.

(30) Ryu, E. K.; Choe, Y. S.; Lee, K. H.; Choi, Y.; Kim, B. T. *J. Med. Chem.* **2006**, *49*, 6111–6119.

(31) (a) Klunk, W. E.; Engler, H.; Nordberg, A.; Wang, Y. M.; Blomqvist, G.; Holt, D. P.; Bergstrom, M.; Savitcheva, I.; Huang, G.; Estrada, F. S.; Ausen, B.; Debnath, M. L.; Barletta, J.; Price, J.; Sandell, C. J.; Lopresti, B. J.; Wall, A.; Koivisto, P.; Antoni, G.; Mathis, C. A.; Långström, B. *Ann. Neurol.* **2004**, *55*, 306–319. (b) Shoghi-Jadid, K.; Small, G. W.; Agdeppa, E. D.; Kepe, V.; Ercoli, L. M.; Siddarth, P.; Read, S.; Satyamurthy, N.; Petric, A.; Huang, S. C.; Barrio, J. R. *Am. J. Geriatr. Psychiatry* **2002**, *10*, 24–35. (c) Verhoeff, N. P. L. G.; Wilson, A. A.; Takeshita, S.; Trop, L.; Hussey, D.; Singh, K.; Kung, H. F.; Kung, M. P.; Houle, S. *Am. J. Geriatr. Psychiatry* **2004**, *12*, 584–595. (d) Kudo, Y.; Okamura, N.; Furumoto, S.; Tashiro, M.; Furukawa, K.; Maruyama, M.; Itoh, M.; Iwata, R.; Yanai, K.; Arai, H. *J. Nucl. Med.* **2007**, *48*, 553–561. (e) Rowe, C. C.; Ackerman, U.; Browne, W.; Mulligan, R.; Pike, K. L.; O'Keefe, G. *Lancet Neurol.* **2008**, *7*, 129–135.

(32) (a) Zhuang, Z. P.; Kung, M. P.; Hou, C.; Ploessl, K.; Kung, H. F. *Nucl. Med. Biol.* **2005**, *32*, 171–184. (b) Chen, X.; Yu, P.; Zhang, L.; Liu, B. *Bioorg. Med. Chem. Lett.* **2008**, *18*, 1442–1445. (c) Serdons, K.; Verduyckt, T.; Cleynhens, J.; Terwinghe, C.; Mortelmans, L.; Bormans, G.; Verbruggen, A. *Bioorg. Med. Chem. Lett.* **2007**, *17*, 6086–6090. (d) Lin, K.-S.; Debnath, M. L.; Mathis, C. A.; Klunk, W. E. *Bioorg. Med. Chem. Lett.* **2009**, *19*, 2258–2262. (e) Zhen, W.; Han, H.; Anguiano, M.; Lemere, C. A.; Cho, C - G.; Lansbury, P. T., Jr. *J. Med. Chem.* **1999**, *42*, 2805–2815. (f) Han, H.; Cho, C - G.; Lansbury, P. T., Jr. *J. Am. Chem. Soc.* **1996**, *118*, 4506–4507. (g) Dezutter, N. A.; Dom, R. J.; De Groot, T. J.; Bormans, G. M.; Verbruggen, A. M. *Eur. J. Nucl. Med.* **1999**, *26*, 1392–1399. (h) Tzanopoulou, S.; Patsis, G.; Sagnou, M.; Pirmettis, I.; Papadopoulos, M.; Pelecanou, M. *Technetium, Rhenium and Other Metals in Chemistry and Nuclear Medicine*; Servici Grafici Editoriali: Padova, 2006; pp 103−104. (i) Ono, M.; Fuchi, Y.; Fuchigami, T.; Kobashi, N.; Kimura, H.; Haratake, M.; Saji, H.; Nakayama, M. *ACS Med. Chem. Lett.* **2010**, *1*, 443–447.

The affinity of complexes **4**−**6** for amyloid plaques of AD was tested following the standard staining procedure applied also in the literature for rhenium complexes.[32b,i] Figure 7 shows the results of the in vitro staining of human post-mortem AD fixed brain sections for complexes **4**−**6** as they appear under the fluorescence microscope. The results of staining with plain curcumin are also presented as a positive control.[6] All complexes bind equally selectively to the plaques, allowing clear visualization of both diffused and dense core ones. It can be seen in Figure 7 that the staining result of the complexes appears comparable to that of curcumin, despite the great difference in their fluorescence intensity (Figure S4 of the Supporting Information). Furthermore, staining of adjacent sections with the typical histological dye thioflavin S showed that complexes **4**−**6** label plaques in a similar way (Figure S6 of the Supporting Information). It is also of interest that the intermediate complex **4** demonstrated binding affinity of equal strength to complexes **5** and **6**, raising it from its usual place as an "intermediate" complex to an independent, potentially bioactive entity, worthy of further evaluation. Overall, the plaque staining results reveal that, despite the direct attachment of curcumin to the rhenium core, the complexes retain the affinity of the mother pharmacophore for β-amyloid plaques, prompting further exploration of their potential as radiodiagnostic agents for AD.

Conclusions

In conclusion, based on the chemistry of the β-diketone acetylacetone with the $[M(CO)_3]^+$ (M = Re, ^{99m}Tc) core, "2 + 1" complexes of the natural β-diketone curcumin were successfully prepared and characterized. The efficient replacement of the water ligand in the intermediate *fac*-$Re(CO)_3(OO)H_2O$ complex by the monodentate ligands imidazole and isocyanocyclohexane offers new prospects in the design of bioactive complexes. Specifically, any molecule linked to the monodentate ligand can in principle be introduced to the β-diketone complex to provide target specificity or to regulate/enhance its properties. Especially in the case of curcumin, the concept of mixed pharmacophore complexes becomes applicable because, in addition to curcumin, a second pharmacophoric molecule may be introduced to the complex as part of the monodentate ligand.

Complexes of curcumin in the literature have been introduced for a variety of biomedical applications, such as antioxidants, antimicrobial, anticancer agents, and so forth. Our work introduces curcumin to the field of radiodiagnosis with SPECT through the preparation of the aqua complex **9** (yield > 90%) and the complexes **10** (yield approximately 30%) and **11** (yield > 90%). The affinity that the Re complexes demonstrate for amyloid plaques makes the in vitro and in vivo biological evaluation of their ^{99m}Tc analogues as potential radiodiagnostic agents for Alzheimer's disease. However, beyond this potential application, the curcumin complexes constitute useful research tools for the exploration of the many biological activities of curcumin, especially in view of the fact that they form a complementary pair of fluorescent (Re) and radioactive (^{99m}Tc) probes and offer the potential of combining microscopic observation with radioimaging results.

Acknowledgment. The authors gratefully acknowledge the support of Professor David Mann of the Greater Manchester Neurosciences Centre, University of Manchester, in kindly providing brain tissue for the staining experiments. They also thank Dr. K. Stamatakis of the Institute of Biology of NCSR "Demokritos" for his help with obtaining the fluorescence spectra in his laboratory. M. Pelecanou gratefully acknowledges financial support by ASPIS Bank, Greece.

Supporting Information Available: ^{1}H and ^{13}C spectra of NMR spectra of imidazole in DMSO-d_6; NOESY spectrum of complex **2**; ^{1}H NMR spectrum of complex **4**; IR spectrum of complex **6**; UV absorbance and fluorescence spectra of curcumin and complexes **5** and **6**; β-amyloid plaque staining with thioflavin S, complex **6**, and curcumin. This material is available free of charge via the Internet at http://pubs.acs.org.